IEEE Access
Multidisciplinary | Rapid Review | Open Access Journal

Received 25 May 2022, accepted 19 June 2022, date of publication 24 June 2022, date of current version 29 June 2022.

Digital Object Identifier 10.1109/ACCESS.2022.3186005

An EGFET Based Common Source Amplifier as a Low-Frequency Instrumentation Amplifier for Sensitivity Measurement on RuO_2 Lactic Acid Biosensor

PO-YU KUO, (Member, IEEE), CHUN-HUNG CHANG, YUNG-YU CHEN, AND WEI-HAO LAI
Graduate School of Electronic Engineering, National Yunlin University of Science and Technology, Douliou 64002, Taiwan

Corresponding author: Po-Yu Kuo (kuopy@yuntech.edu.tw)

This work was supported in part by the Ministry of Science and Technology, Taiwan, under Grant MOST 110-2221-E-224-051 and Grant MOST 109-2221-E-224-013; and in part by the Taiwan Semiconductor Research Institute (TSRI) (technical support).

ABSTRACT In this study, a low-frequency instrumentation amplifier (LFIA) integrated with an extended-gate field-effect transistor (EGFET) is presented to realize the simplicity common source amplifier (CSA) structure. The proposed EGFET CSA was developed by the 0.18-μm CMOS process technology of Taiwan Semiconductor Manufacturing Company (TSMC). The EGFET CSA has low frequency and noise immunity function, and it can effectively output the response signal, with good stability and effectively improve the sensitivity, not susceptible to environmental factors, easy to replace, and low cost. Moreover, the simple circuit design of the EGFET CSA was used to analyze the sensing characteristics and to improve the stability of the ruthenium dioxide (RuO_2) lactic acid (LA) biosensor. Therefore, the EGFET CSA is suitable for LA detection. The simple process of the EGFET CSA was used to analyze the sensing characteristics and to improve the stability of the ruthenium dioxide (RuO_2) lactic acid (LA) biosensor. An arrayed potentiometric LA biosensor based on the RuO_2 thin film was proposed and manufactured in this study. The experimental results indicated that the EGFET CSA as a low-frequency instrumentation amplifier has achieved a good sensitivity (53.41mV/mM) and satisfactory linearity (0.997) on the RuO_2 LA biosensor as compared with the V-T measurement system.

INDEX TERMS Extended gate field-effect transistor (EGFET), common source amplifier (CSA), ruthenium dioxide (RuO_2), lactic acid (LA), low-frequency instrumentation amplifier (LFIA).

I. INTRODUCTION

The ion-sensitive field-effect transistor (ISFET) is the first biosensor field-effect transistor (BioFET) sensor based on metal-oxide-semiconductor field-effect transistor (MOSFET). Piet Bergveld [1] proved the ISFET in 1970. It has the same basic structure as MOSFET but replaces the metal gate equipped with an ion-sensitive membrane, electrolyte solution, and reference electrode. The mechanism of ISFET is that the potential of the oxide surface is affected by hydrogen ions that cause the channel current to change. As the charges on the surface of the sensing layer increase, the electron concentration of the resulting channel increased accordingly. In 1983, J Spiegel [2] proposed an extended-gate field-effect transistor (EGFET) structure. EGFET retains the metal of the MOSFET gate and separates the sensing area from the gate of MOSFET. The extended gate consists of a substrate and a sensing window as a gate of the MOSFET in the analyte solutions. Moreover, it has the advantages of chemical sensing area, electrical distinction, easier packaging than ISFET. The EGFET has some inherent advantages, such as a simpler manufacturing process, less influence by optical illumination, operating temperature, a one-time gate, not being susceptible to chemical contamination, and having good noise immunity. These advantages make EGFET a potential device structure in biotechnology so that it was less affected by light, easy to change the shape of the sensing film, and easy to relocate the sensing film of the sensing area [3].

The associate editor coordinating the review of this manuscript and approving it for publication was Chih-Yu Hsu.

The sensors are considered to be an important vehicle for sustainable development. To solve the world's health problems, decentralized diagnostic systems will become sophisticated sensors, achieving miniaturization, versatility, and artificial intelligence. The sensors have also been discussed in depth by humans [4]. Effective detection of electrochemical [5], [6], medical [7], pharmaceutical [8] and fluorescent detection [9]. In recent years, it has also been applied to wearable, intelligent and portable methods to change the traditional measurement methods [10], [11]. Staden *et al.* analyzed electrochemical sensors in biomedicine and promoted the development of miniaturized and automated sensing technologies [5]. Chung *et al.* developed electrochemical aptamer-based (EAB) sensors that provide continuous, real-time measurements of specific molecular concentrations. At present, the EAB sensor has been proved to be able to distinguish and measure the plasma concentration of a variety of drugs and metabolites in the vein of live rats, making a major breakthrough in the application of sensors [6]. Sharma *et al.* synthesized molecular imprinting Polymer (MIP) and measured Klebsiella pneumonia (K. Pneumonia) Bacteria by electrochemical technique. Due to the simple polymer matrix and good biocompatibility, the synthesis of MIP has attracted much attention [7]. Kocheril *et al.* coupled two lasers to a planar optical waveguide for multiple fluorescence detection. By measuring in this way, the multiplex capability of the sensor can be proved [9]. Glasco *et al.* described in depth the milestones of 3D printing technology and its common medical applications in wearable and physical sensors, with advantages including precise control of the shape and spatial dimensions of sensor elements, reduced manufacturing time, and mass production [10]. Santos *et al.* explore the application of electrochemical techniques to metals in archaeological, cosmetic, food, fuel, and gunshot residue samples. The metal and semi-metal content provides different information for analyzing samples. It can be widely used to observe the age, pollution caused to the human body, environmental damage, and criminal evidence [12]. Fan *et al.* combined sensors with nano-antibodies for direct detection of target analytes in cell lysates, and combined with Graphite felt showed perfect mechanical integrity, which is suitable for wearable sensors [13]. The performance of the sensor depends on the sensitivity, selectivity, stability, and repeatability, and the readout circuit and sensing material are combined to make it more efficient.

In nanomaterials, two-dimensional (2D) materials have a high surface area and adjustable physicochemical properties. Traditional two-dimensional materials such as graphene and its derivatives, metal disulfide, and molybdenum disulfide have been explored as sensing materials. However, commercial development is constrained by complex functionalities, structural defects, hydrophobic, and electrical trade-offs [14]. Two-dimensional transition metal carbides, called MXenes. It was an emerging class of two-dimensional materials with extensive applications, especially in electrochemical energy storage [15]. The hydrophilicity of MXene combined with its metal conductivity and surface redox reaction is the key to efficient pseudocapacitor storage in the MXene electrode. The RuO_2 has high conductivity, large proton-induced pseudocapacitance, and high oxygen overpotential [16]. In addition, the RuO_2 was applied to transparent conductive materials with high thermodynamic stability on nanomaterials. The electrical transmission characteristics of nanosheet devices were improved by surface treatment of metal nanoparticles [17], therefore the RuO_2 was selected.

In recent years, several transparent conductive materials have been developed such as SnO_2, ZnO, CuO, In_2O_3, RuO_x, and InGaZnO [18]-[26], have been widely used in pH sensors. Compared with other metal oxides, the ruthenium dioxide (RuO_2) has fast proton transfer, high redox reversibility, high specific capacitance, low resistivity over ions, good electrical conductivity, and high thermal and electrical stability [27]. Therefore, it becomes a great candidate for energy storage applications. RuO_2 film has been applied in glucose, pH sensor, chloride ion sensor, urea, and uric acid detection sensing film [24], [28]–[31]. In this study, RuO_2 is deposited on the substrate by a radio frequency (RF) sputtering system with a RuO_2 target. The lactic acid (LA) is a key energy metabolite of several approximately from 0.5 mM to 1.5 mM [32]. The LA is not physiological pathways in the heart, brain, and skeletal muscle. The concentration range of LA in the adult blood is only found in the aforementioned places an organic compound. It is widely distributed in the human body [33], [34]. The enzyme sensor manufacturing process is simple; it can be stored at room temperature. The enzyme sensor is susceptible to interference and has a narrow concentration range. Therefore, in this study, a LA sensor is developed with easy structure and has a wide concentration range.

Existing researchers tend to use commercially available MOSFETs as EGFET devices and instead focus on the development of the sensing window [22], [35], [36]. Taking advantage of these works, in this study, we propose a novel measurement method that is emphasized simplicity and effectiveness as well. To realize this purpose, a CMOS EGFET has been designed and used as resistance to construct a simple common source amplifier (CSA) typology in the proposed biosensor measurement system shown in Figure 1. In this structure, the gate of EGFET connected to the sensing window had a LA RuO_2 sensing film. This well-designed reference electrode EGFET was used to measure the sensitivity and linearity.

II. EXPERIMENTAL DESIGN

A. MATERIALS

The RuO_2 target (99.95% purity) was purchased from Ultimate Materials Technology Co., Ltd (Hsinchu County, Taiwan), the polyethylene terephthalate (PET) substrate was purchased from Zencatec Corporation (Tao-Yuan City, Taiwan). The silver paste was purchased from Advanced Electronic Material Inc. (Tainan City, Taiwan), and the epoxy thermosetting polymer was bought from Sil-More Industrial, Ltd. (New Taipei City, Taiwan). The LA solution,

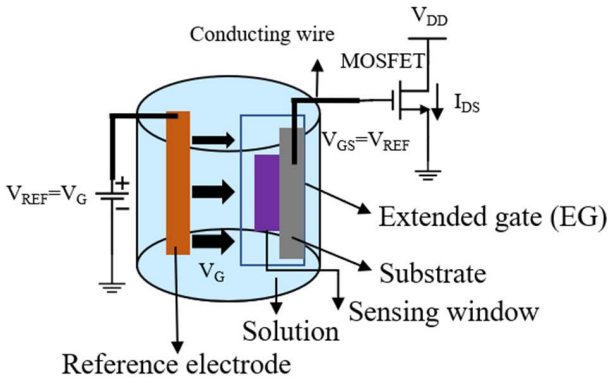

FIGURE 1. The proposed simple EGFET CSA biosensor measurement architecture.

the β-Nicotinamide adenine dinucleotide hydrate, and the L-Lactic Dehydrogenase from rabbit muscle were purchased from J. T. Baker Corp. (St. Louis, MO, USA). The γ-aminopropyl triethoxysilane (γ-APTES), and glutaraldehyde were purchased from Sigma-Aldrich Corp. (St. Louis, MO, USA). The phosphate-buffered saline (PBS) (pH7.0) was bought from AppliChem GmbH Crop (Darmstadt, Germany) which was used to mix LA solutions at different concentrations, and the deionized water (D.I.) was used for the preparation of the aqueous solutions and substrate cleaning (resistivity =18.4MΩ cm^{-1}).

B. DESIGN OF THE EGFET OF THE MOSFET DEVICE AND THE INSTRUMENTATION AMPLIFIER

A low-frequency instrumentation amplifier (LFIA) integrated with an EGFET was proposed and developed by the 0.18-μm TSMC CMOS process technology. Moreover, we proposed an arrayed potentiometric LA biosensor based on the RuO_2 thin film to determine LA. The measurement architecture of the EGFET includes a MOSFET, a conducting wire, an extended gate of RuO_2 LA biosensor, a reference electrode, and a solution as shown in Figure 1. According to the Gouy-Chapman-Stern model, the equivalent circuit can be described as shown in Figure 2. V_{REF} is the voltage from the reference electrode and C_{Gouy} is the capacitance of the diffusion layer. The electrolyte solution changes with the concentration of the electrolyte solution. C_{Helm} is the capacitance between the metal oxide and the electrolyte solution. The potential of the reference electrode was practically around 3mV [37].

The extended gate includes a substrate and a sensing window as a gate of the MOSFET in the solution. The reference electrode is used as an enhancement to provide a scanning potential for the extended gate in the solution, and the $V_{GS} = V_{REF}$. Therefore, the $I_{DS} - V_{DS}$ relation in the saturation region and linear region of the MOSFET is as follows (1) and (2) [21].

$$I_{DS(linear)} = \mu_n C_{OX} \frac{W}{L}[(V_{REF} - V_{T(EGFET)})V_{DS} - \frac{1}{2}V_{DS}^2] \quad (1)$$

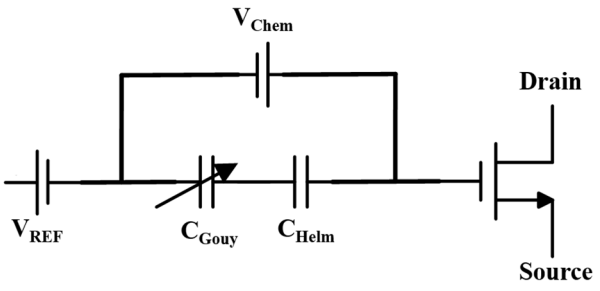

FIGURE 2. The completed fabrication process equivalent circuit of the arrayed RuO_2 LA biosensor.

TABLE 1. Parameters for preparation of the RuO_2 thin film.

Target	RuO_2
RF Power (W)	50
Deposition Pressure (mTorr)	10
Gas flow (Ar:O_2,sccm)	10:1
Deposition (min)	30

$$I_{DS(saturation)} = \mu_n C_{OX} \frac{W}{2L}[(V_{REF} - V_{T(EGFET)})^2] \quad (2)$$

The work function of the reference electrode was ΦM/q, the reference electrode potential was E_{REF}, and the surface dipole potential of the electrolyte was χ^{sol}. The I_{DS}-V_{DS} curve indicated that EGFET had different saturation I_{DS} at different LA concentrations. The threshold voltage (V_T) of the EGFET can be described by the formula (3) [21].

$$V_{T(EGFET)} = V_{T(MOSFET)} - \frac{\Phi M}{q} + E_{REF} + X^{Sol} - \Phi \quad (3)$$

C. FABRICATION OF THE RUO2 LA BIOSENSOR

There are six sensing windows and two REs on a PET substrate with a size of 30 mm × 35 mm. The schematic diagram of the completed fabrication process for the RuO_2 LA biosensor was shown in Figure 3 and depicted as follows. First, the silver adhesive was printed onto the PET substrate using screen-printing technology, to provide the conducting wire and reference electrode. Secondly, the RuO_2 then was deposited on the silver adhesive by the RF sputtering system. The sputtering parameters for the RuO_2 thin film was shown in Table 1 [31]. Thirdly, we used epoxy resin as insulation encapsulation and baked it in the oven for 1 hour. Finally, the lactase was dropped on the RuO_2 thin film.

In addition, the dehydrogenase needs to add coenzyme, the synthesis of lactate dehydrogenase (LDH), nicotinamide adenine dinucleotide (NAD^+), and PBS [38]. The synthetic ratio of lactase was LDH 2 mg, NAD^+ 2 mg, and PBS 200 μL. APTES and glutaraldehyde were added as a protective layer and adhesive. Soaking the sensors in the LA

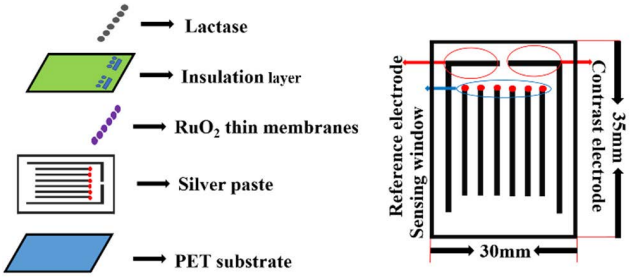

FIGURE 3. The completed fabrication process for the arrayed RuO_2 LA biosensor with the schematic diagram.

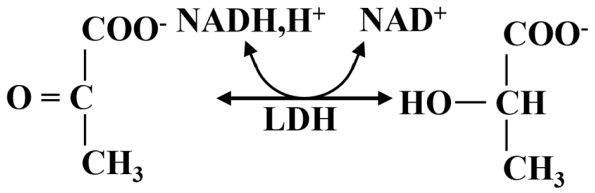

FIGURE 4. The sensing mechanism of LA.

solutions, the concentration range of the prepared solutions were 0.2 mM, 0.7 mM, 1.3 mM, 2 mM, 3 mM, and 5 mM, the test time was 60 seconds. The LDH is an H^+ transfer oxidoreductase. The function of this enzyme is to catalyze the reversible conversion of LA to pyruvate while reducing NAD^+ to NADH, where the NADH can then produce H^+. Through the hydrogen ions accumulating on the surface of the sensing film, the different LA concentrations will produce different response voltages. The sensing mechanism of LA is shown in Figure 4. As shown in formulas (4) and (5) [39]:

$$Lactate + NAD^+ \rightarrow Pyruvate + NADH + H^+ \quad (4)$$

$$NADH \rightarrow NAD^+ + H^+ + 2e^- \quad (5)$$

Yates *et al.* [40] proposed site binding model that denoted three kinds of adsorbed states O^-, OH^{2+} and OH were generated on the sensing film when it was immersed in solution. H^+ was easy to be adsorbed on the sensing film. Thus, forming an interface potential on the sensing film. The RuO_2 lactate biosensor detected the H^+ ion concentrations to obtain the response voltage.

The potentiometric biosensor was used to measure response voltage through the change of hydrogen ions in LA concentrations to different solutions. The response voltage was used to determine the concentration of LA. The sensing mechanism of the RuO_x film of the obtained redox reaction was shown in equation (6) [41].

$$Ru\,(OH)_3 \leftrightarrow Ru\,(OH)_2\,O^- + H^+ \quad (6)$$

The potential of the electrode is given by a modified version of the Nernst equation (7) [24], [41], [42].

$$E = E^0 - \frac{RT}{F} In \frac{Ru(OH)_3}{[RuO_2][H^+]} = (E^0 - \frac{RT}{F} In \frac{Ru(OH)_3}{[RuO_2]}) - \frac{RT}{F} In[H^+] \quad (7)$$

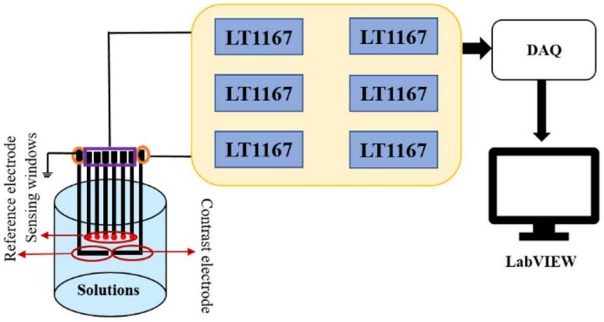

FIGURE 5. The V-T measurement system.

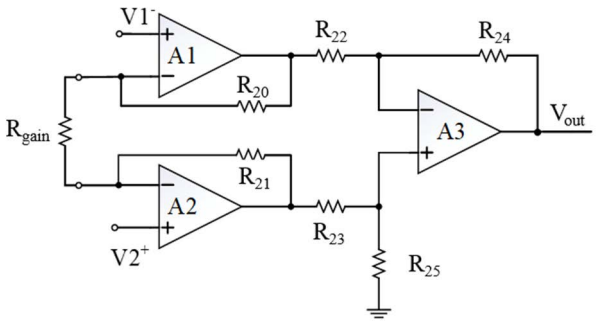

FIGURE 6. The circuit schematic of the instrumentation amplifier.

In this redox reaction, E^0 is the potential of the reference electrode, R is the universal gas constant of 8.31 J/(Kmol), T is the absolute temperature, and F is the Faraday constant 96485.33 C /mol. The H^+ represents the activity of Ru^{III}, Ru^{IV}, in absolute temperature, respectively.

To compare, the sensing characteristics of the array LA biosensor were measured through the traditional V-T measurement system as shown in Figure 5. The measurement system was composed of a data acquisition card (DAQ), an instrumental amplifier, and LabVIEW software [43], [44]. The input voltage of the sensing windows and the reference electrode was transmitted to the IA (LT1167), and the output voltage was transmitted to the DAQ to convert the analog signal into a digital signal. The LabVIEW software was used to collect the measurement data and aggregate it for analysis and compare with the proposed EGFET CSA.

D. AN LFIA DESIGN INTEGRATED WITH EGFET

A standard instrumental amplifier (IA) consists of three operational amplifiers and six resistances. This circuit has the advantages of high gain, high common-mode rejection ratio (CMRR), low frequency, and low output impedance. The gain of the IA depended on R_{gain}. If R_{gain} is removed, the gain of the IA was 1. The resistances R_{22}, R_{24}, and operational amplifier A3 form a standard differential amplifier circuit. In the IA, the resistances $R_{20} = R_{21}$, $R_{22} = R_{23}$ and $R_{24} = R_{25}$. The commonly used IA circuit as shown in Figure 6. The

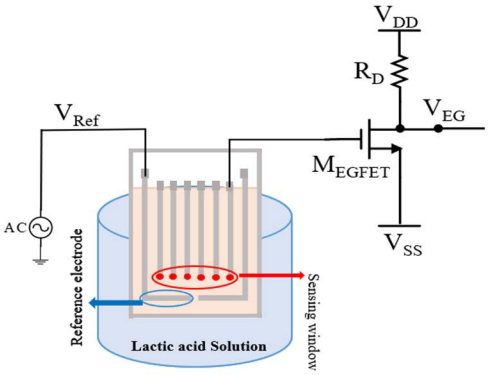

FIGURE 7. The proposed simple circuit schematic of the EGFET CSA.

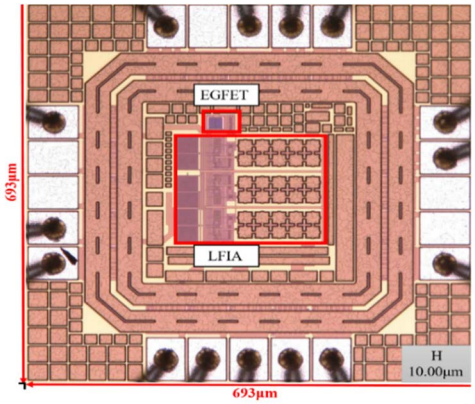

FIGURE 8. Die photograph of the proposed LFIA and an EGFET.

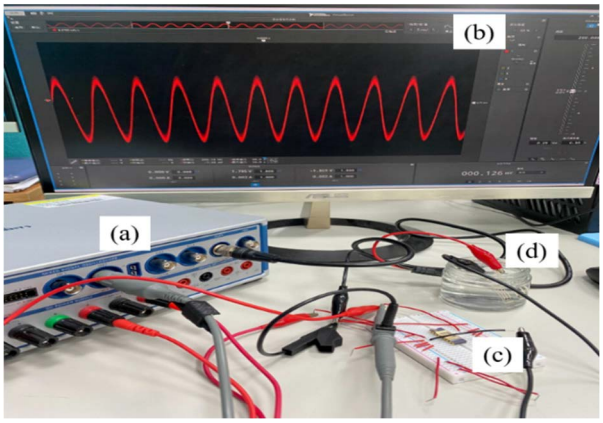

FIGURE 9. Measurement pieces of equipment, (a) Virtual Bench, (b) Response voltages waveform, (c) LFIA integrated with an EGFET, (d) RuO_2 LA biosensor.

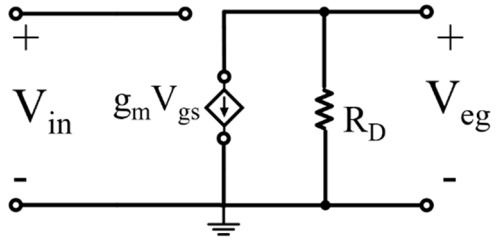

FIGURE 10. The small-signal equivalent circuit of M_{EGFET}.

gain of the circuit is expressed by equation (8).

$$Av = \frac{V_{out}}{V_2 - V_1} = (\frac{2R_{20}}{R_{gain}})\frac{R_{24}}{R_{22}} \tag{8}$$

The circuit schematic of the simple EGFET CSA with a RuO_2 LA sensing window is shown in Figure 7. The gate of the M_{EGFET} was connected to the RuO_2 LA sensing window, the drain was connected to the resistor R_D, which is connected to the V_{DD}, and the source was connected to the V_{SS}. The transistor M_{EGFET} was operated in the saturated region. The area of the whole chip was 693 μm $\times$ 693μm, as shown in Figure 8. To observe the I_D-V_D curve of the EGFET, the V_{DD} was set to 1.8V. The gate, source, and drain of the designed EGFET were connected to the semiconductor parameter analyzer (4156, Keysight, USA).

III. RESULTS AND DISCUSSION

A. SENSING ANALYSIS OF EGFET CSA

The characteristics measuring equipment allocation of the EGFET CSA are depicted as follows. A Virtual Bench (VB-8034, NI, USA) was used to measure the properties of the EGFET CSA. The Virtual Bench consists of a signal generator, an oscilloscope, and a power supply instrument. An LFIA was integrated with an EGFET in a chip and implemented by TSMC using their 0.18-μm CMOS process technology. The length and width of EGFET were 10 μm by 20 μm. The actual allocation diagram of the EGFET CSA measurement system is shown in Figure 9. The V_{DD} and V_{SS} were set as 1.5 V and -1.5 V. And, the EGFET CSA was measured by Virtual Bench. A common source circuit of a FET serves as a path for signal input and output. The signals are input from the gate and output at the drain. The MOSFET small-signal equivalent circuit of M_{EGFET} between input and output as shown in Figure 10. The current through the equivalent impedance of the circuit ($r_{out}||R_D$) generates an amplified output voltage. The A_V and g_m were the voltage gain and the mutual conduction of the CSA, respectively [45].

To measure the biosensor characteristics, an A_C signal of 0.2 V was given to V_{Ref}, and soaked the sensors in the LA solution, the concentration range of the prepared solutions were 0.2 mM, 0.7 mM, 1.3 mM, 2 mM, 3 mM, and 5 mM. Figure 11 showed that the sensitivity was 53.41 mV/mM and the linearity was 0.997 when measured by EGFET CSA. Figure 12 showed the peak voltage variations at different concentrations. It is noted that the response voltage increases with higher concentration.

Next, the sensing characteristics of the array LA biosensor were measured using the traditional V-T measurement system. From the results shown in Figure 13, the biosensor had an average sensitivity of 32.93 mV/mM and linearity

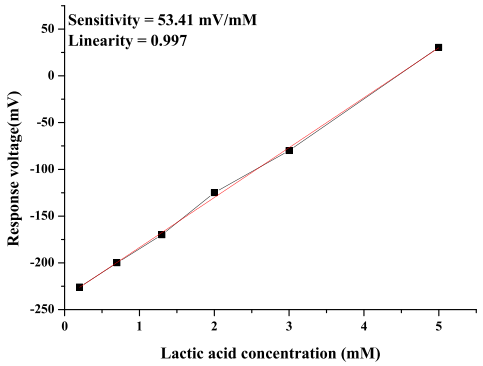

FIGURE 11. The sensitivity and linearity of RuO_2 LA biosensor with sensing window based on EGFET.

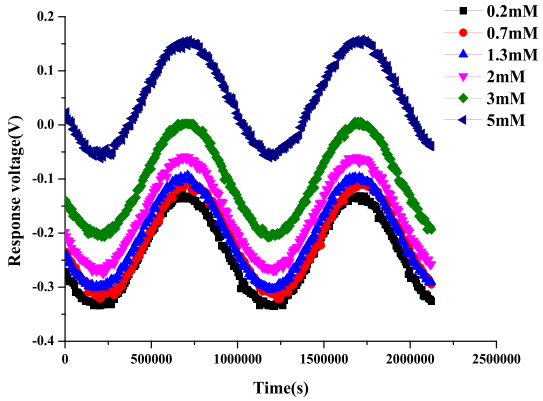

FIGURE 12. The response voltages of the EGFET CSA at different concentrations.

TABLE 2. The sensing characteristics of the two measurement systems.

	Sensitivity	Linearity
EGFET CSA (This work)	53.41 mV/mM	0.997
V-T measurement system	32.93 mV/mM	0.996

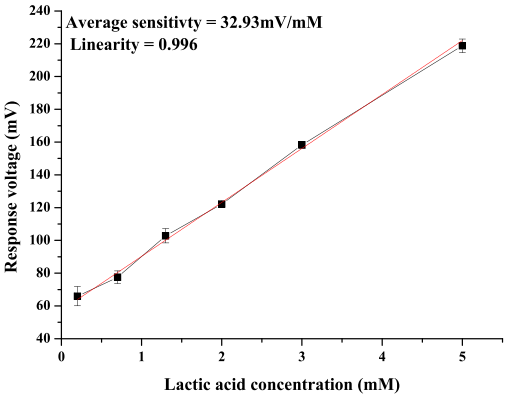

FIGURE 13. The average sensitivity and linearity of the RuO_2 LA biosensor.

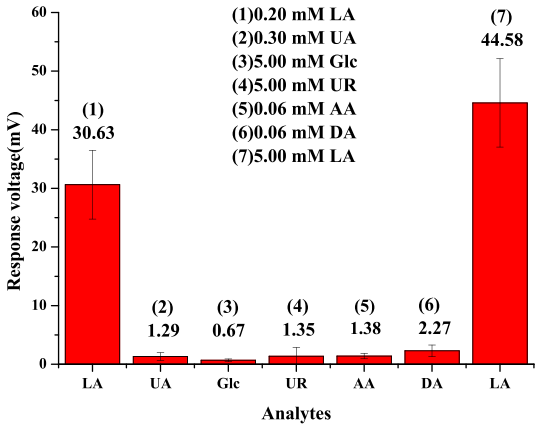

FIGURE 14. The selectivity of the RuO_2 LA biosensor.

of 0.996. Table 2 showed the sensing characteristics of the two measuring systems' comparing results. The proposed LA biosensor with an EGFET CSA achieved a better average sensitivity (53.41 mV/mM) while keeping good linearity (0.997).

To the specificity of the RuO_2 LA biosensor, a selectivity test was performed. We added five different interfering substances which exist in the human body including uric acid (UA), glucose (Glc), urea (UR), ascorbic acid (AA), and dopamine (DA). Firstly, we immersed the biosensor into the PBS solution for 30 seconds. Then we added interfering substances, LA of 0.20 mM, UA of 0.30 mM, Glc of 5.00 mM, UR of 5.00 mM, AA of 0.06 mM, DA of 0.06 mM, and LA of 5.00 mM. The concentrations of these interfering substances were the same as that in the human body.

The concentrations of these interfering substances were the same as that in the human body [46]. The biosensors are required to detect specific analytes. The biosensor response does not change with other substances [47]. The selectivity refers to the ability of a biosensor to detect specific analytes in the environment with other chemicals or contaminants [47]. Since the LA biosensor is an enzyme sensor, it is necessary to react with LA in the analyte more accurately in the selective experiment to verify that the sensor has a large response voltage to LA.

The selectivity of the RuO_2 LA biosensor was shown in Figure 14. The LA biosensor had high specificity for LA. After adding other interfering substances, the response voltage was changed slightly. However, the response voltage changed significantly when the LA was added. TABLE 3 showed the response voltages with different interferences.

Repeatability is the repeated measurement of the same subject using the same method in the same environment. By applying this method, we can know whether the same results are obtained using the same measurement method [48]. In this study, the LA sensor was immersed in 5 mM LA solution and measured for six times. According to Figure 15, the average response voltage of LA is 212.99 mV$\pm$1.17 mV. The percentage relative standard

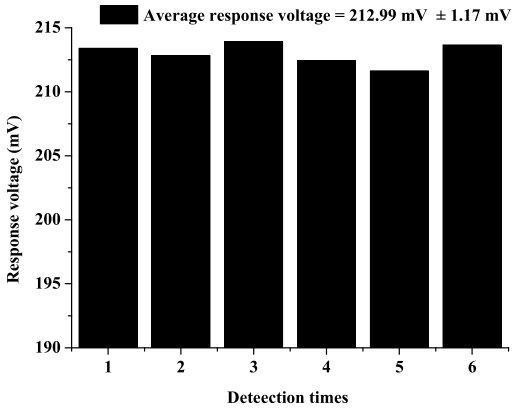

FIGURE 15. Repeatability of the RuO_2 LA biosensor.

TABLE 3. The response voltages under different interferences.

Interferences	Response Voltage (mV)	Standard deviation (mV)
0.20 mM LA	30.63	5.87
0.30 mM UA	1.29	0.64
5.00 mM Glc	0.67	0.99
5.00 mM UR	1.35	1.49
0.06 mM AA	1.38	0.46
0.06 mM DA	2.27	0.12
5.00 mM LA	44.58	7.52

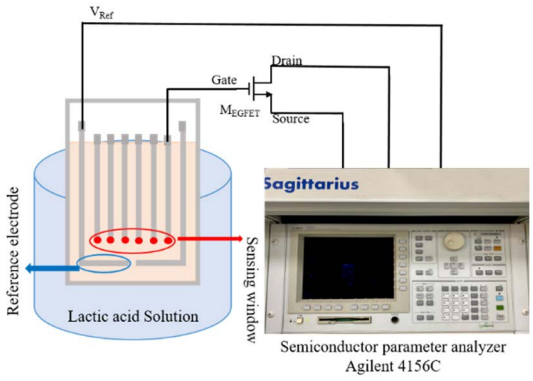

FIGURE 16. The measurement setup of RuO_2 LA EGFET.

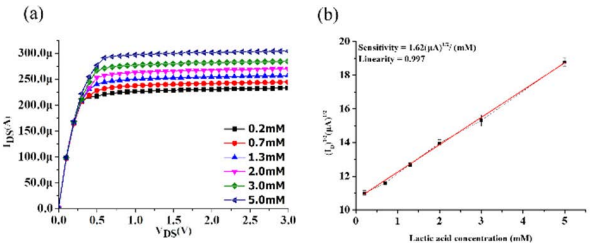

FIGURE 17. The I_D-V_D curves (a) at different LA concentrations (b) The average sensitivity and the linearity of EGFET while V_D = 2V.

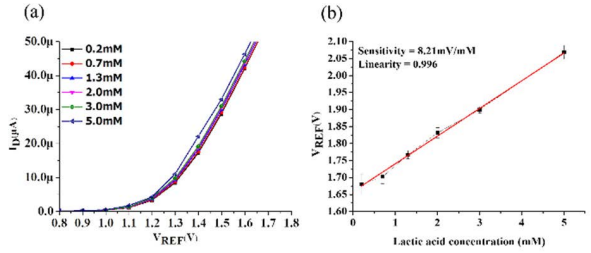

FIGURE 18. The I_D-V_{REF} curves (a) RuO_2 LA EGFET at different LA concentrations (b) The sensitivity and the linearity of RuO_2 LA EGFET.

TABLE 4. The I_D-V_D and I_D-V_{REF} measurement analysis.

	LA concentrations (mV/mM)	Response voltage (mV)	Response current $\mu A^{1/2}$/ (mM)	Standard Deviation (mV)
I_D-V_D	0.2		10.99	0.16
	0.7		11.59	0.31
	1.3		12.72	0.14
	2		13.96	0.22
	3		15.31	0.33
	5		18.77	0.25
I_D-V_{REF}	0.2	1.68		0.03
	0.7	1.70		0.02
	1.3	1.76		0.01
	2	1.83		0.01
	3	1.89		0.01
	5	2.06		0.02

deviation (RSD%) can be determined by Equation (9):

$$RSD = \frac{Standard\ deviation}{Arithmetic\ mean} \times 100\% \tag{9}$$

Thus, RSD% of the proposed LA sensor is 0.18% and this sensor is very stable.

The semiconductor parameter analyzer was used to measure the properties of EGFET with a RuO_2 sensor immersed in the concentration of LA shown in Figure 16. And, Figure 17(a) showed the I_D-V_D curve at different LA concentrations while the V_G = 2.0 V, V_D = 0-3.0 V. In the I_D-V_D curve, we can see that EGFET had different saturation I_D at different LA concentrations. Figure 17(b) showed the average sensitivity and the linearity of EGFET while the V_D = 2.0 V. The horizontal axis was the concentrations of LA solutions; the vertical axis was $(I_D)^{1/2}$. From the experiment results, the biosensor has a current sensitivity of 1.62 $(\mu A)^{1/2}$/ (mM) and linearity of 0.997. Figure 18(a) showed the I_D-V_{REF} curve for the different LA concentrations when V_{REF} was scanned from 0.8 V to 1.8 V and V_D was fixed to 2.0 V. In Figure 18(b), the LA EGFET has the sensitivity of 8.21 mV/mM and the linearity of 0.996. The current sensitivity can be derived from Equation (10)[21]. The voltage sensitivity can be determined by Equation (11) [21].

TABLE 5. The sensing characteristics of various LA biosensors.

Sensing architecture	Film	Linear range (mV/mM)	Sensitivity (mV/mM)	Linearity	Ref.
LT1167	LDH/NAD^+/RuO_2	0.2 - 5	32.93	0.996	In this study
EGFET CSA	LDH/NAD^+/RuO_2	0.2 - 5	53.41	0.997	In this study
Electrochemical sensor	LOD/Si_3N_4	1 - 6	20.00	N/A	[49]2013
LT1167	LDH/NAD^+/IGZO	0.3 - 3	56.09	0.998	[50]2017
LT1167	LDH/NAD^+/MB_s/GPTS/GO/NiO	0.2 - 3	45.40	0.992	[51]2018
LT1167	LDH/NAD^+/GPTS/NiO	0.2 - 3	38.21	0.992	[32]2018
Electrochemical sensor	LOD/MnO_2 NPs/SiO_2	8×10^{-3} - 6	16.80	N/A	[52]2005

Current sensitivity

$$= \frac{\sqrt{I_{DS(saturation)_2}} - \sqrt{I_{DS(saturation)_1}}}{Concentration_2 - Concentration_1} = \frac{Change\ in\ \sqrt{I_{DS(saturation)}}}{Change\ in\ Concentration} \quad (10)$$

Voltage sensitivity

$$= \frac{V_{T(EGFET)_2} - V_{T(EGFET)_1}}{Concentration_2 - Concentration_1} = \frac{Change\ in\ V_{T(EGFET)_1}}{Change\ in\ Concentration} \quad (11)$$

We measured the same concentration repeatedly for 5 times and calculated its error bars. To show the range of error, the standard deviations of I_D-V_D curves and I_D-V_{REF} curves were added in Table 4. During the measurements, the results of I_D-V_D curves and I_D-V_{REF} curves were not affected by noise, and the signal was fairly stable in the measurement system. According to Pan's research [20], when EGFET is measured by SPA, the voltage and current changes of the LA sensor at different concentrations were displayed by scanning fixed voltage and current. Therefore, the sensing performance of the RuO_2 LA EGFET can be accurately tested during measurements.

Table 5 showed the comparing results of various LA biosensors concerning their sensitivity, linearity, and associated concentration ranges. In a previous study, Lupu *et al.* [49] constructed a microsensor and platinum microelectrode, combining potentiometer and galvanometer technology. The sensitivity of 20 mV/mM was obtained in the concentration range of 1 - 6 mM. By using LDH/NAD^+ titration on IGZO film, the measurement range was from 0.3 mM to 3 mM, with an average sensitivity of 56.09 mV /mM and linearity of 0.998 [50]. In Lupu's study, although their LA biosensor has a wide measurement range, and he discovered that LDH/NAD^+/MBs/GPTS/GO/NiO made by GO and MBs can improve biocompatibility and biocatalyst [51], the effect of toxicity and linearity is still not as good as our EGFET CSA biosensor instrument amplifier. In Lupu's work, the NiO thin films fixed by LDH/NAD^+ and crosslinking agent GPTS had relatively stable average sensitivity and linearity [32]. This LA biosensor was based on an enzyme field-effect transistor (ENFET) and constructed by RuO_2 LA biosensors. The experimental results showed that the average sensitivity of the traditional I-V measuring system was 32.93 mV/mM and the linearity was 0.996 by LT1167, while the average sensitivity of the EGFET CSA was 53.41 mV/mM and the linearity was 0.997. It can be seen that EGFET CSA had good stability and had good noise immunity. By applying our measurement structure, good sensitivity and linearity can be achieved more simply way without the need for further modifications such as magnetic beads and bovine serum albumin [50], [53].

IV. CONCLUSION

In this study, an EGFET CSA as a LFIA and a RuO_2 LA biosensor was proposed and manufactured. Through the experiments, the EGFET CSA and the V-T measurement system were used to measure the sensitivity characteristics of the LA biosensor. The average sensitivity was 53.41mV/mM and the linearity was 0.997 when EGFET CSA was applied. This measurement system has better average sensitivity and linearity compared with the V-T measurement system. To measure the specificity of the sensor, the selectivity experiment was carried out, and it was proved that there were drastic changes in LA. This device does not require the addition of any modifiers to improve the sensing characteristics but can show good sensing characteristics, indicating that the sensor had good stability compared with previous works.

REFERENCES

[1] P. Bergveld, "Development of an ion-sensitive solid-state device for neurophysiological measurements," *IEEE Trans. Biomed. Eng.*, vol. BME-17, no. 1, pp. 70–71, Jan. 1970, doi: 10.1109/TBME.1970.4502688.
[2] J. van der Spiegel, I. Lauks, P. Chan, and D. Babic, "The extended gate chemically sensitive field effect transistor as multi-species microprobe," *Sens. Actuators*, vol. 4, pp. 291–298, May 1983, doi: 10.1016/0250-6874(83)85035-5.
[3] S. Sheibani, A. M. Ionescu, and P. Norouzi, "Extended gate field effect transistor based sensor for detection of trace amounts of antidepressant drug," *IEEE Access*, vol. 8, pp. 198010–198020, 2020, doi: 10.1109/ACCESS.2020.3034691.
[4] A. P. Turner, "Perspective—An age of sensors," *ECS Sensors Plus*, vol. 1, Apr. 2022, Art. no. 010001, doi: 10.1149/2754-2726/ac5523.
[5] R. I. Stefan-Van Staden, "Perspective—Challenges in biomedical analysis: From classical sensors to stochastic sensors," *ECS Sensors Plus*, vol. 1, no. 1, Apr. 2022, Art. no. 011603, doi: 10.1149/2754-2726/ac5ddd.

[6] J. Chung, L. Sepunaru, and K. W. Plaxco, "On the disinfection of electrochemical aptamer-based sensors," *ECS Sensors Plus*, vol. 1, no. 1, Apr. 2022, Art. no. 011604, doi: 10.1149/2754-2726/ac60b2.

[7] R. Sharma, G. Lakshmi, A. Kumar, and P. Solanki, "Polypyrrole based molecularly imprinted polymer platform for klebsiella pneumonia detection," *ECS Sensors Plus*, vol. 1, no. 1, Apr. 2022, Art. no. 010603, doi: 10.1149/2754-2726/ac612c.

[8] J. Wang, "Amperometric biosensors for clinical and therapeutic drug monitoring: A review," *J. Pharmaceutical Biomed. Anal.*, vol. 19, pp. 47–53, Feb. 1999, doi: 10.1016/S0731-7085(98)00056-9.

[9] P. A. Kocheril, K. D. Lenz, and H. Mukundan, "Total internal reflection of two lasers in a single planar optical waveguide," *ECS Sensors Plus*, vol. 1, no. 2, May 2022, Art. no. 021601, doi: 10.1149/2754-2726/ac6523.

[10] D. L. Glasco, A. Sheelam, N. H. Ho, A. M. Mamaril, M. King, and J. G. Bell, "Editors' choice—Review-3D printing: An innovative trend in analytical sensing," *ECS Sensors Plus*, vol. 17, pp. 1–17, Apr. 2022, doi: 10.1149/2754-2726/ac5c7a.

[11] A. Scott, R. Pandey, S. Saxena, E. Osman, Y. Li, and L. Soleymani, "A smartphone operated electrochemical reader and actuator that streamlines the operation of electrochemical biosensors," *ECS Sensors Plus*, vol. 1, no. 1, Apr. 2022, Art. no. 014601, doi: 10.1149/2754-2726/ac5fb3.

[12] F. D. S. Santos, L. V. da Silva, P. V. S. Campos, C. de Medeiros Strunkis, C. M. G. Ribeiro, and M. O. Salles, "Recent advances of electrochemical techniques in food, energy, environment, and forensic applications," *ECS Sensors Plus*, vol. 1, no. 1, Apr. 2022, Art. no. 013603, doi: 10.1149/2754-2726/ac5cdf.

[13] R. Fan, Y. Li, K. W. Pank, J. Du, L. H. Chang, E. R. Strieter, and T. L. Andrew, "A strategy for accessing nanobody-based electrochemical sensors for analyte detection in complex media," *ECS Sensors Plus*, vol. 1, no. 1, Apr. 2022, Art. no. 010601, doi: 10.1149/2754-2726/ac5b2e.

[14] V. Chaudhary, A. K. Kaushik, H. Furukawa, and A. Khosla, "Towards 5th generation AI and IoT driven sustainable intelligent sensors based on 2D MXenes and borophene," *ECS Sensors Plus*, vol. 34, pp. 1–34, Apr. 2022, doi: 10.1149/2754-2726/ac5ac6.

[15] Q. Jiang, N. Kurra, M. Alhabeb, Y. Gogotsi, and H. N. Alshareef, "All pseudocapacitive MXene-RuO_2 asymmetric supercapacitors," *Adv. Energy Mater.*, vol. 8, no. 13, Jan. 2018, Art. no. 1703043, doi: 10.1002/aenm.201703043.

[16] C.-C. Hu, K.-H. Chang, M.-C. Lin, and Y.-T. Wu, "Design and tailoring of the nanotubular arrayed architecture of hydrous RuO_2 for next generation supercapacitors," *Nano Lett.*, vol. 6, no. 12, pp. 2690–2695, Nov. 2006, doi: 10.1021/nl061576a.

[17] J. Kim, S. Youn, J. Y. Baek, D. H. Kim, S. Kim, W. Lee, H. J. Park, J. Kim, D. W. Chun, S.-S. Park, J. W. Roh, and J. Kim, "Modulation of conductivity and contact resistance of RuO_2 nanosheets via metal nano-particles surface decoration," *Nanomaterials*, vol. 11, no. 9, p. 2444, Sep. 2021, doi: 10.3390/nano11092444.

[18] S.-J. Young, L.-T. Lai, and W.-L. Tang, "Improving the performance of pH sensors with one-dimensional ZnO nanostructures," *IEEE Sensors J.*, vol. 19, no. 23, pp. 10972–10976, Dec. 2019, doi: 10.1109/JSEN.2019.2932627.

[19] A. T. Erozan, G. Y. Wang, R. Bishnoi, J. Aghassi-Hagmann, and M. B. Tahoori, "A compact low-voltage true random number generator based on inkjet printing technology," *IEEE Trans. Very Large Scale Integr. (VLSI) Syst.*, vol. 28, no. 6, pp. 1485–1495, Jun. 2020, doi: 10.1109/TVLSI.2020.2975876.

[20] T.-M. Pan, C.-H. Lin, and S.-T. Pang, "Structural and sensing characteristics of NiO_X sensing films for extended-gate field-effect transistor pH sensors," *IEEE Sensors J.*, vol. 21, no. 3, pp. 2597–2603, Feb. 2021, doi: 10.1109/JSEN.2020.3027060.

[21] A. K. Mishra, D. K. Jarwa, B. N. Mukharjee, A. Kumar, S. Ratan, and S. Jit, "CuO nanowire-based extended-gate field-effect-transistor (FET) for pH sensing and enzyme-free/receptor-free glucose sensing applications," *IEEE Sensors J.*, vol. 20, no. 9, pp. 5039–5047, May 2020, doi: 10.1109/JSEN.2020.2966585.

[22] A. K. Singh, A. Pandey, and P. Chakrabarti, "Fabrication, characterization, and application of CuO nano wires as electrode for ammonia sensing in aqueous environment using extended gate-FET," *IEEE Sensors J.*, vol. 21, no. 5, pp. 5779–5786, Mar. 2021, doi: 10.1109/JSEN.2020.3042659.

[23] H. Kim, Y. S. Rim, and J. Kwon, "Evaluation of metal oxide thin-film electrolyte-gated field effect transistors for glucose monitoring in small volume of body analytes," *IEEE Sensors J.*, vol. 20, no. 16, pp. 9004–9010, Aug. 2020, doi: 10.1109/JSEN.2020.2988269.

[24] K. Singh, B.-S. Lou, J.-L. Her, S.-T. Pang, and T.-M. Pan, "Super Nernstian pH response and enzyme-free detection of glucose using sol-gel derived RuO_X on PET flexible-based extended-gate field-effect transistor," *Sens. Actuators B, Chem.*, vol. 298, Nov. 2019, Art. no. 126837, doi: 10.1016/j.snb.2019.126837.

[25] S.-J. Young, Y.-J. Chu, and Y.-L. Chen, "Enhancing pH sensors performance of ZnO nanorods with Au nanoparticles adsorption," *IEEE Sensors J.*, vol. 21, no. 12, pp. 13068–13073, Jun. 2021, doi: 10.1109/JSEN.2021.3062857.

[26] S.-K. Cho and W.-J. Cho, "Effect of forming gas annealing on SnO_2 sensing membranes in high-performance silicon-on-insulator extended-gate field-effect transistors," *Thin Solid Films*, vol. 706, Jul. 2020, Art. no. 138083, doi: 10.1016/j.tsf.2020.138083.

[27] M. Manuraj, J. Chacko, K. N. N. Unni, and R. B. Rakhi, "Heterostructured MoS_2-RuO_2 nanocomposite: A promising electrode material for supercapacitors," *J. Alloys Compounds*, vol. 836, Sep. 2020, Art. no. 155420, doi: 10.1016/j.jallcom.2020.155420.

[28] S.-C. Tseng, T.-Y. Wu, J.-C. Chou, Y.-H. Liao, C.-H. Lai, S.-J. Yan, and T.-W. Tseng, "Investigation of sensitivities and drift effects of the arrayed flexible chloride sensor based on RuO_2/GO at different temperatures," *Sensors*, vol. 18, no. 2, p. 632, Feb. 2018, doi: 10.3390/s18020632.

[29] A. Sardarinejad, D. K. Maurya, and K. Alameh, "The effects of sensing electrode thickness on ruthenium oxide thin-film pH sensor," *Sens. Actuators A, Phys.*, vol. 214, pp. 15–19, Apr. 2014, doi: 10.1016/j.sna.2014.04.007.

[30] P.-Y. Kuo, Z.-X. Dong, and Y.-Y. Chen, "The stability analysis of potentiometric urea biosensor under microfluidic system and remote measurement," *IEEE Trans. Instrum. Meas.*, vol. 70, pp. 1–13, 2021, doi: 10.1109/TIM.2021.3075036.

[31] P.-Y. Kuo and Y.-Y. Chen, "A novel low unity-gain frequency and low power consumption instrumentation amplifier design for RuO_2 uric acid biosensor measurement," *IEEE Trans. Instrum. Meas.*, vol. 70, pp. 1–9, Feb. 2021, doi: 10.1109/TIM.2021.3060571.

[32] J.-C. Chou, S.-J. Yan, Y.-H. Liao, C.-H. Lai, J.-S. Chen, H.-Y. Chen, C.-Y. Wu, and Y.-X. Wu, "Reaction of NiO film on flexible substrates with buffer solutions and application to flexible arrayed lactate biosensor," *Microelectron. Rel.*, vol. 83, pp. 249–253, Apr. 2018, doi: 10.1016/j.microrel.2017.06.036.

[33] F. Torabi, K. Ramanathan, P, -O, Larsson, L. Gorton, K. Svanberg, Y. Okamoto, B. Danielsson, and M. Khayyami, "Coulometric determination of NAD^+ and NADH in normal and cancer cells using LDH, RVC and a polymer mediator," *Talanta*, vol. 50, no. 4, pp. 787–797, Nov. 1999, doi: 10.1016/S0039-9140(99)00134-4.

[34] J. S. Narayanan and G. Slaughter, "Lactic acid biosensor based on lactate dehydrogenase immobilized on au nanoparticle modified microwire electrode," *IEEE Sensors J.*, vol. 20, no. 8, pp. 4034–4040, Apr. 2020, doi: 10.1109/JSEN.2019.2963405.

[35] K. K. Hussain, N. G. Gurudatt, M. H. Akhtar, K.-D. Seo, D.-S. Park, and Y.-B. Shim, "Nano-biosensor for the *in vitro* lactate detection using bi-functionalized conducting polymer/N, S-doped carbon; the effect of αCHC inhibitor on lactate level in cancer cell lines," *Biosensors Bioelectron.*, vol. 155, May 2020, Art. no. 112094, doi: 10.1016/j.bios.2020.112094.

[36] C.-C. Yang, K.-Y. Chen, and Y.-K. Su, "TiO_2 nano flowers based EGFET sensor for pH sensing," *Coatings*, vol. 9, no. 4, p. 251, Apr. 2019, doi: 10.3390/coatings9040251.

[37] W. Guan, X. Duan, and M. A. Reed, "Highly specific and sensitive non-enzymatic determination of uric acid in serum and urine by extended gate field effect transistor sensors," *Biosensors Bioelectron.*, vol. 51, pp. 225–231, Jan. 2014, doi: 10.1016/j.bios.2013.07.061.

[38] N. Miscourides and P. Georgiou, "ISFET arrays in CMOS: A head-to-head comparison between voltage and current mode," *IEEE Sensors J.*, vol. 19, no. 4, pp. 1224–1238, Feb. 2019, doi: 10.1109/JSEN.2018.2881499.

[39] J.-C. Chou, D.-G. Wu, S.-C. Tseng, C.-C. Chen, and G.-C. Ye, "Application of microfluidic device for lactic biosensor," *IEEE Sensors J.*, vol. 13, no. 4, pp. 1363–1370, Apr. 2013, doi: 10.1109/JSEN.2016.2609605.

[40] E. D. Yates, S. Levine, and W. T. Healy, "Site-binding model of the electrical double layer at the oxide/water interface," *J. Chem. Soc., Faraday Trans., Phys. Chem. Condens. Phases*, vol. 1, vol. 170, pp. 1807–1818, 1973, doi: 10.1039/F19747001807.

[41] W. Lonsdale, S. P. Shylendra, S. Brouwer, M. Wajrak, and K. Alameh, "Application of ruthenium oxide pH sensitive electrode to samples with high redox interference," *Sens. Actuators B, Chem.*, vol. 273, pp. 1222–1225, Nov. 2018, doi: 10.1016/j.snb.2018.07.022.

[42] P. Kurzweil, "Precious metal oxides for electrochemical energy converters: Pseudocapacitance and pH dependence of redox processes," *J. Power Sources*, vol. 190, no. 1, pp. 189–200, May 2009, doi: 10.1016/j.jpowsour.2008.08.033.
[43] Y. Yadav, R. Roshan, S. Umashankar, D. Vijayakumar, and D. P. Kothari, "Real time simulation of solar photovoltaic module using labview data acquisition card," in *Proc. Int. Conf. Energy Efficient Technol. Sustainability*, Apr. 2013, pp. 512–523, doi: 10.1109/ICEETS.2013.6533438.
[44] P.-Y. Kuo and Z.-X. Dong, "A new calibration circuit design to reduce drift effect of RuO_2 urea biosensors," *Sensors*, vol. 19, no. 20, p. 4558, Oct. 2019, doi: 10.3390/s19204558.
[45] U. Dutta, M. K. Soni, and M. Pattanaik, "Simulation study of hetero dielectric tri material gate tunnel FET based common source amplifier circuit," *AEU Int. J. Electron. Commun.*, vol. 99, pp. 258–263, Feb. 2019, doi: 10.1016/j.aeue.2018.12.004.
[46] J.-C. Chou, S.-H. Lin, P.-Y. Kuo, C.-H. Lai, Y.-H. Nien, T.-Y. Lai, and T.-Y. Su, "A sensitive potentiometric biosensor using MBs-AO/GO/ZnO membranes-based arrayed screen-printed electrodes for AA detection and remote monitoring," *IEEE Access*, vol. 7, pp. 105962–105972, 2019, doi: 10.1109/ACCESS.2019.2931773.
[47] C. Karunakaran, R. Rajkumar, and K. Bhargava, "Introduction to biosensors," in *Biosensors and Bioelectronics*. Amsterdam, The Netherlands: Elsevier, Jul. 2015, doi: 10.1016/B978-0-12-803100-1.00001-3.
[48] A. Zanobini, B. Sereni, M. Catelani, and L. Ciani, "Repeatability and reproducibility techniques for the analysis of measurement systems," *Measurement*, vol. 86, pp. 125–132, May 2016, doi: 10.1016/j.measurement.2016.02.041.
[49] A. K. Diallo, L. Djeghlaf, L. Mazenq, J. Launay, W. Sant, and P. T. Boyer, "Development of pH-based ElecFET biosensors for lactate ion detection," *Biosens. Bioelectron.*, vol. 40, no. 1, pp. 291–296, Feb. 2013, doi: 10.1016/j.bios.2012.07.063.
[50] J.-C. Chou, H.-Y. Chen, Y.-H. Liao, C.-H. Lai, M.-S. Huang, J.-S. Chen, S.-J. Yan, and C.-Y. Wu, "Sensing characteristic of arrayed flexible indium gallium zinc oxide lactate biosensor modified by magnetic beads," *IEEE Sensors J.*, vol. 17, no. 18, pp. 5920–5926, Sep. 2017, doi: 10.1109/jsen.2017.2731864.
[51] J.-C. Chou, S.-J. Yan, Y.-H. Liao, C.-H. Lai, Y.-X. Wu, and C.-Y. Wu, "Remote detection for glucose and lactate based on flexible sensor array," *IEEE Sensors J.*, vol. 18, no. 8, pp. 3467–3474, Apr. 2018, doi: 10.1109/JSEN.2018.2805292.
[52] J. J. Xu, W. Zhao, X. L. Luo, and H. Y. Chen, "A sensitive biosensor for lactate based on layer-by-layer assembling MnO_2 nanoparticles and lactate oxidase on ion-sensitive field-effect transistors," *Chem. Commun.*, vol. 6, pp. 792–794, Feb. 2005, doi: 10.1039/B416548A.
[53] N. Thomas, I. Lähdesmäki, and B. A. Parviz, "A contact lens with an integrated lactate sensor," *Sens. Actuators B, Chem.*, vol. 162, no. 1, pp. 128–134, Feb. 2012, doi: 10.1016/j.snb.2011.12.049.

PO-YU KUO (Member, IEEE) was born in Taichung, Taiwan, in 1980. He received the M.S. and Ph.D. degrees in electrical engineering from The University of Texas at Dallas, in 2006 and 2011, respectively. In 2013, he joined the Department of Electronic Engineering, National Yunlin University of Science and Technology, Yunlin, Taiwan, where he is currently an Associate Professor. His research interests include the analog circuits, power management circuits, analog circuit model analysis, and biosensors measurement.

CHUN-HUNG CHANG was born in Yunlin, Taiwan, in January 1998. He received the bachelor's degree from the Department of Electronic Engineering, Minghsin University of Science and Technology, Hsinchu, Taiwan, in 2020. He is currently pursuing the master's degree with the Graduate School of Electronic Engineering, National Yunlin University of Science and Technology, Yunlin. His research interests include EGFET biosensor applications and microfluidics measurement systems.

YUNG-YU CHEN was born in Kaohsiung, Taiwan, in July 1997. He received the bachelor's degree from the Department of Electronic Engineering, National Yunlin University of Science and Technology, Yunlin, Taiwan, in 2019, where he is currently pursuing the master's degree with the Graduate School of Electronic Engineering. His research interests include analog readout circuit and noise cancellation circuit for the biosensors measurement systems.

WEI-HAO LAI was born in Hsinchu, Taiwan, in August 1998. He received the bachelor's degree from the Department of Electrical Engineering, National Chin-Yi University of Technology, Taichung, Taiwan, in 2020. He is currently pursuing the master's degree with the Graduate School of Electronic Engineering, National Yunlin University of Science and Technology, Yunlin, Taiwan. His research interests include temperature compensation circuits for biosensors and EGFET biosensor applications.